RESEARCH ARTICLE

Characteristics and application of new grouting materials for poor geology with rich water

Yuanli Bai[1, *], Chao Tao[2]

[1]Department of Civil Engineering, [2]Department of Plant Engineering, Sichuan College of Architectural Technology, Deyang, Sichuan, China

Received: July 5, 2023; **accepted:** September 1, 2023.

The poor water-rich geology in underground engineering construction is easy to cause geological disasters such as water inrush, sand gusher, and sand flow, which have adverse effects on engineering progress and personnel safety. Grouting is an effective means to control poor geology with rich water, but the traditional cement grouting material has some issues such as long coagulation time and low strength. Therefore, this study proposed a new grouting material based on graphene oxide and fly ash. Through the systematic analysis of the material, the working performance of the material was verified. Considering the fluidity, stability, setting time, and economy of the slurry, 0.03% graphene oxide and 20% fly ash were mixed into the slurry, which not only ensured the excellent properties of the slurry, but also realized the resource of fly ash. The mechanical property analysis of the material indicated that, when the fly ash content was 10%, the flexural strength increased by 8.11% and the compressive strength increased by 6.01% at the age of 28 days. When the fly ash content was 20%, the flexural strength was improved by 4.39%. The compressive was enhanced by 8.13%. The experimental results verified the feasibility of the grouting material. A low carbon, green, and high-performance grouting material is very important for the treatment of water-rich crushing zones. This study provided a new solution for the grouting reinforcement project of water-rich fracture zone, which owned the essential research significance and values.

Keywords: rich water; poor geology; grouting material; graphene oxide; fly ash.

[*]**Corresponding author:** Yuanli Bai, Department of Civil Engineering, Sichuan College of Architectural Technology, Deyang 618000, Sichuan, China. Email: xiaobai20131107@126.com.

Introduction

With the continuous acceleration of the process of urbanization construction, urban traffic is becoming increasingly tense. In the construction of urban rail transportation, it is usually faced with difficult problems such as complicated hydrogeological conditions and frequent engineering geological disasters [1]. Among those problems, the poor cementation ability, low strength, high fluidity, and poor stability of water-rich geology often cause water inrush, sand gusher, and sand flow disasters, which brings economic losses to the project construction and also poses a threat to the life safety of the working force [2]. Therefore, how to adopt effective technical means to improve the underground engineering characteristics of aquifer fracture zone and reduce engineering accidents and risks is very challenging [3]. Grouting technology is an effective treatment method for poor geology with rich water. Grouting material (GM) influences the quality of the whole project. Traditional GM has some issues such as low stone rate, long coagulation time, and low strength. Fly ash (FA) and graphene

oxide (GO) have been proven to improve the properties of cement-based composites [4, 5].

As one of the most common ways to prevent water inrush in surrounding rock, grouting has become an important technical means to treat the broken zone in underground engineering. GM is an essential factor affecting the reinforcement effect, which has been studied by many researchers. Li, *et al*. synthesized a new GM in view of the shortcomings of simple to dilute and difficult to set and tested the fluidity of the GM and determined the optimal solid-liquid ratio. The results showed that this material had excellent performance in blocking water inrush and put forward innovation for GM with certain enlightening significance [6]. Another study proposed a GM based on the characteristics of broken surrounding rock with stronger plasticity and resistance to denaturation [7]. Zhang, *et al*. synthesized a new GM based on dynamic thermodynamic analysis. The material was mainly used for emergency rescue and could achieve a better water response. However, this material still had many limitations [8]. From the perspective of improving grouting technology, relevant numerical simulations for grouting were carried out. The critical conditions for effective grouting were investigated and the results showed that reasonable setting of grouting parameters could enhance the overall effect of grouting, which could improve the grouting effect to a certain extent [9]. Yu, *et al*. found that the existing GM could not meet the advantages of high strength and convenient pumping, so a modified GM was developed with a good application effect on roadway restoration and reinforcement engineering. However, the production cost of this GM was high [10]. The diffusion behavior of GM was investigated through the test of the sealed hole grouting, which laid a foundation for further exploration of the characteristics of GM [11]. Zhang, *et al*. found that the traditional GM had shortcomings, so a mixed GM of polypropylene fiber, polyvinyl alcohol fiber, and basalt fiber was proposed, which could significantly improve the ductility of such materials and had good application value [12]. Some researchers believed that fiber-reinforced cement-based GM was popular in coal mining because of their toughness and electrical conductivity. Therefore, a GM with good flexibility, good dispersion, and tensile strength was developed with significantly improved electrical conductivity [13]. Yang, *et al*. studied the effects of kaolin content on mechanical properties, setting time, and rheology of GM, while the compressive strength of the proposed GM increased with the increase of kaolin content [14]. For the perspective of improving the smoothness, comfort, and safety of railway lines, Huang, *et al*. developed a GM for the reconstruction of the ballastless track pumping area with good relevant dynamic test results [15].

A lot of studies have been done by domestic researchers on grouting materials and grouting reinforcement theory. However, in view of the current grouting treatment of poor geology with water-rich, the grouting materials still need to be further studied. In addition, there is a large research space on the properties of GO and FA grouting materials. Therefore, aiming at the problem of poor grouting effect of traditional cement grouting materials, a new GO-FA grouting material was proposed in this study, and its characteristics were analyzed to improve the grouting effect of underground engineering under poor geological conditions with rich water. This study would provide a new solution for the grouting reinforcement project of water-rich fracture zone with both essential research significance and values.

Materials and Methods

Synthesis of the new grouting material (GM)

The main raw materials of the new GM included Shijing Ordinary Portland Cement (Po42.5) (Zhujiang Cement Co., Ltd. Guangzhou, Guangdong, China); FA Grade II fly ash (FA) obtained from Yuanheng Environmental Protection Engineering Co., LTD. in Henan province, China with an irregularly sized spherical particle of about 5-30 μm and a smooth surface;

graphene oxide (GO) prepared by Suzhou Carbon Feng Graphene Technology Co., LTD (Suzhou, Jiangsu, China) using $KMnO_4$ as the oxidant; polycarboxylic acid superplasticizer (PC) (Guangzhou Xika Building Materials Co., LTD, Guangzhou, Guangdong, China) as the water reducer; Type 8604 accelerator (Hongfu building admixture factory, Dongying, Shandong, China); and tap water that met the requirements of JGJ63-2006 "Concrete Water Standard". The control variable method was applied to explore the influences of different proportions of the raw materials on the working characteristics of the new GM with the cement amounts ranged from 200 - 400 g, water consumption ranged from 160 - 400 g, FA from 0 - 200 g, GO from 4 - 60 mL, 0.2% optimal water reducing agent, and 0.5%, 0.8%, 1.0%, 1.2%, and 1.5% five different concentrations of accelerator. The setting times of the slurry under different water-cement ratio and different accelerator content were tested under the experimental temperature of 25°C. The cement-based grouting slurry was prepared by slowly mixing cement, FA, and accelerator in NJ-160 mixer (Shaoxing Experiment Instrument Equipment Co., Ltd., Shaoxing, Zhejiang, China) at 62 ± 5 rpm for 150 seconds before adding water reducer, GO, and water to start the automatic stirring mode at 62 ± 5 rpm for 125 s, pause for 10 s, then 125 ± 10 rpm for 120 s. The prepared slurry was then poured into a square test mold with a side length of 50 mm until fully filled. The final volume of the obtained mixture was 125 cm^3. After solidification for 24 hours, the sample was taken out and placed in a standard curing box with relative humidity greater than 95% and temperature at 20 ± 2°C for 28 days. The flatness error of each surface of the sample should not exceed 0.05 mm, while the height error should be less than 0.3 mm. The properties of new GM were analyzed from the aspects of water extraction rate, setting time, fluidity, flexure strength, compressive strength, erosion resistance, permeability resistance, resistance and damping ratio [16].

Determination of characteristics of new GM

The water evolution rate of the GM reflected the stability of the grout. The water evolution rates of different grout ratio were observed by using a 250 mL cylinder. Briefly, 200 mL slurry was put into the 250 mL measuring cylinder and sealed with a plastic film to facilitate calculation. After resting for 2 hours, the cement particles were settled steadily and the water in the mud no longer increased. The reading of the upper and lower mud interfaces was then recorded while ensuring that the errors of three reads were within 1% before recording the average value. The slurry water extraction rate was calculated as the water conversion rate obtained by taking 180 ml of slurry as follows:

$$B = \left[(180 - h) / 180 \right] \times 100\% \quad (1)$$

where *B* was the water conversion rate. *h* was the scale reading of the interface between the clean water surface and the lower slurry after standing still. Similarly, 180 mL of cement slurry was poured into a measuring cylinder, and the scale of the lower part of the measuring cylinder was recorded after curing the sample for 24 hours. The stone formation rate was calculated as:

$$S = \left(H / 180 \right) \times 100\% \quad (2)$$

where *S* was the stone formation rate. *H* was the scale reading of the stone body after 24 hours of resting. In addition, the setting time of the slurry was also an essential index to reflect its stability. The initial setting time referred to the time when the slurry was just prepared until its molding began to decrease. The final setting time referred to the time when the slurry completely lost its plasticity [17]. The initial setting times were evaluated every 15 minutes before the initial setting state, while the final setting times were evaluated every 5 minutes near the final setting state. The flow test of the slurry was carried out by measuring the slurry diffusion degree after 30 seconds and calculating the average value. The bending strength of the stone body of the slurry referred to the ultimate load that the material

could bear per unit area under the action of bending pressure. It was calculated as:

$$f_s = \left(1.5F_sL\right) / \left(bh^2\right) \quad (3)$$

where f_s was the flexural strength. F_s was the flexural failure load. b was the width of the stone. h was the height of the stone. The compressive strength of stone body represented the gelling ability of cement hardening to a certain age and was a crucial index to characterize the physical characteristics of stone. The compressive strength was calculated as follows:

$$f_c = F_c / A \quad (4)$$

where f_c was the compressive strength of the stone. F_c was the compressive failure load of the stone. A was the compression area of the stone. The stone's impermeability was the impermeability of the GM in the rock layer, which was particularly important for the water-rich and poor geological underground engineering. It could be calculated as:

$$K = \left(aD^2\right) / 2TH \quad (5)$$

where K was the relative permeability coefficient. D was the depth of deep water. H was the water pressure expressed by the height of the water column. T was the time for adding water pressure. a was the water absorption. As a new type of GM, its erosion resistance was also considered. Corrosion resistance reflected the durability and service life of GM and could be used to consider the economy and environmental protection of underground engineering. The erosion resistance was calculated as follows:

$$K_f = \left(F_e / F_0\right) \times 100\% \quad (6)$$

where K_f was the erosion resistance coefficient. F_e was the eroded stone's compressive strength value. F_0 was the eroded stone's flexural strength at the corresponding age under standard curing conditions. The calculation for the resistivity of the stone was then shown below:

$$\rho = 2\pi\alpha\left(U / I\right) \quad (7)$$

where ρ was the resistivity value. a was the electrode spacing. U was the voltage measured by the two electrodes. I was the applied current. The damping properties that represented the ability of an object to return to its excited state after being excited of the stones were also measured in this study by using tapping method.

The working characteristics of GO-FA new GM

Based on the composition-property-structure-structure relationship of ordinary Portland cement (PO), FA, and GO, this study analyzed the working characteristics of the new GM systematically. The yield stress and plastic viscosity were the main factors. The yield stress referred to the maximum stress resisting the plastic deformation of the grout, which was related to the deformation ability of the newly mixed grouting grout. Its time equation was shown below.

$$\tau = \tau_0 + ae^{bt} \quad (8)$$

where τ_0 was the initial yield stress. a and b were the coefficients of the slurry itself. t was the duration of the test. Plastic viscosity referred to the mud in each layer flow formed a viscous resistance in the opposite direction of the mud flow, which was a property to prevent the flow of mud and was expressed as:

$$\eta = ce^{kt} + \eta_0 \quad (9)$$

where η_0 was the initial viscosity. c was the coefficient of the slurry itself. k was the viscosity coefficient of the slurry. t was the duration of the test. In the actual construction of underground engineering in water-rich and poor geological areas, the GM's flexural strength and compressive strength are also important indicators. Assuming that the elastic modulus of

the stone body of the GM was *E*, then the equation (10) would be the expression of elastic modulus and compressive strength.

$$E = A \cdot f_c^{1/2} \quad (10)$$

where $f_c^{1/2}$ was compressive strength. *A* was a constant usually related to the density of the material. The smaller the density was, the smaller the *A* value was. In actual projects, the grouting effect was crucial to project governance [2, 18]. During the hardening process of grouting slurry, the change of resistivity was closely related to the strength of stone body. The fitting function expression of resistivity and age was shown in Equation (11).

$$\rho = \rho_0 - C \cdot e^{(-t/D)} \quad (11)$$

where ρ was the resistivity of the stone body. ρ_0 was the initial resistivity. *C* and *D* were both resistivity coefficients. *t* was the age of the stone body. This equation could be used to characterize the relationship between the resistivity of serous hardened stones and their age, and to predict the resistivity of the stones [19]. The relationship between compressive strength and resistivity of different proportioning stones was shown as follows:

$$f_c = \alpha\rho - f_0 \quad (12)$$

where f_c was compressive strength. ρ was resistivity. f_0 was initial compressive strength. α was compressive strength coefficient. By combining Equations (11) and (12), Equation (13) was obtained below, which represented the relationship between the compressive strength of the stone body and the age.

$$f_c = \alpha\rho - C\alpha \cdot e^{\left(-\frac{t}{D}\right)} - f_0 \quad (13)$$

This equation could be used to predict the age of compressive strength of GM stones. The equation for calculating the damping characteristics of the stone body was as follows:

$$A_k / A_{k+1} = V_k / V_{k+1} = a_k / a_{k+1} = e^{-\xi\omega T} \quad (14)$$

where A_k / A_{k+1} was the ratio of amplitudes of two adjacent stones. V_k / V_{k+1} was the ratio of two adjacent speeds. a_k / a_{k+1} was the ratio of two adjacent accelerations. ξ was the damping ratio of the GM. ω was the undamped circular frequency. *T* was the vibration response time. The damping ratio was calculated as:

$$\xi = \frac{1}{2i\pi} \ln\left(a_n / a_{n+i}\right) \quad (15)$$

where ξ was the damping ratio of the material. a_n and a_{n+1} were *n* and *n+1* peak accelerations, respectively.

Results and discussion

Stability analysis of GO-FA new GM

The stability of GM was tested according to the characteristics of poor geological grouting reinforcement treatment with rich water. The stability of the slurry was mainly manifested as good fluidity, low water evolution rate, and controllable solidification time under full agitation. In this study, the stability of cement slurry was analyzed by using macroscopic indexes including fluidity, water extraction rate, and setting time. To ensure the fluidity of the slurry, polycarboxylic acid superplasticizer was utilized to adjust the fluidity with the slurry flow of 323 ± 6 mm and 300 g cement. By changing the total amount of water, the optimal amount of water reducing agent was determined to be 0.2% by the method of gradual approximation. The results of FA and GO for grout flow were shown in Figure 1. When the FA content was less than 21%, the fluidity increased rapidly with the increase of the FA content with the fluidity increased by 25.77% and 8.39% in PC-0 and PC-0.2 conditions, respectively. When the FA content reached 21%,

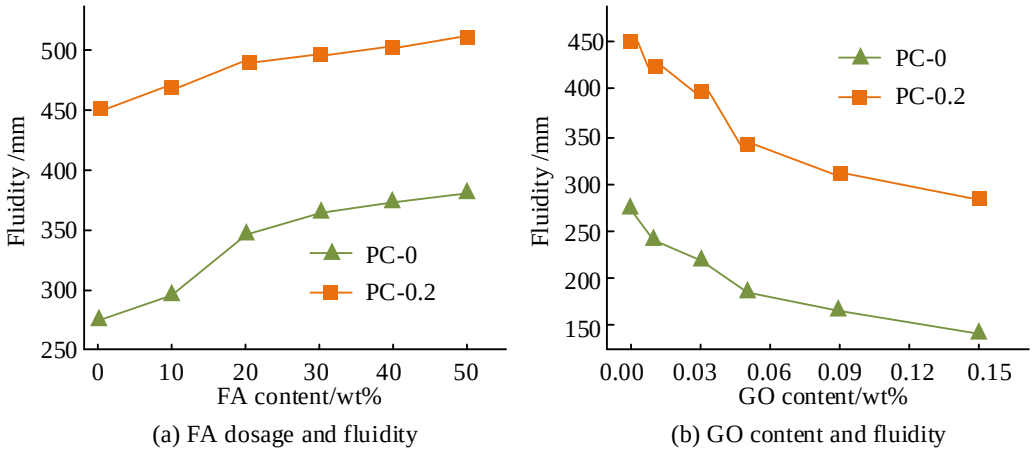

Figure 1. FA and GO contents on slurry fluidity. PC-0 indicated that no water reducer was added. PC-0.2 indicated the addition of 0.2% polycarboxylic acid water reducer.

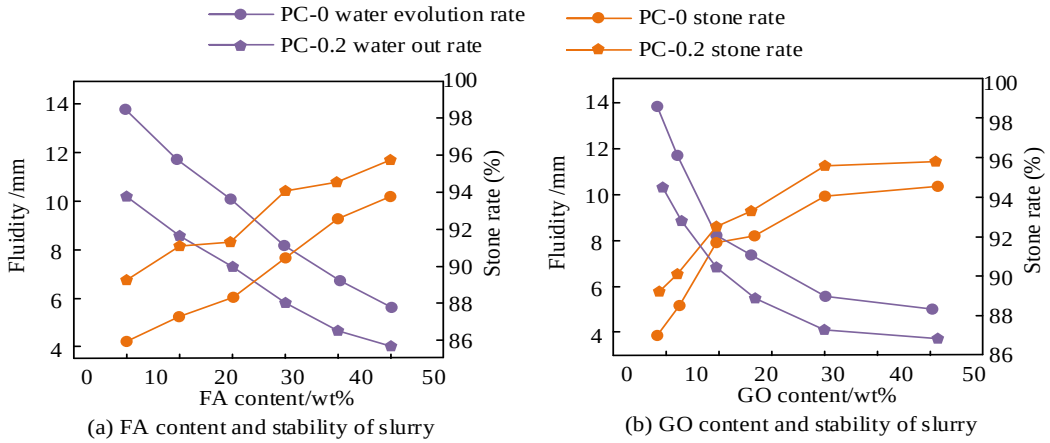

Figure 2. FA and GO contents on slurry stability.

the slurry fluidity gradually stabled. Therefore, the optimal content of FA was 21%. When GO content was less than 0.05%, the flow loss rate was large (Figure 1b). However, when GO reached 0.05%, the flow loss rates of PC-0 and PC-0.2 were 32.69% and 24.19%, respectively. The main reason that GO reduced the flow of slurry was that it had a large surface area and formed a flocculating structure in the slurry while absorbing free water. The structure enclosed the free water and hindered the reaction between the free water and the glue. Figure 2 showed the test results of FA and GO for slurry stability. When FA content increased, the water evolution rate of the grout showed a linear decline trend, while the setting rate gradually increased. In the case of PC-0, the water extraction rate decreased from 10.19% to 3.89%, while, in the case of PC-0.2, the water extraction rate decreased from 13.79% to 5.69%. The water evolution rate of PC-0.2 was obviously higher than that of PC-0. When GO content increased, the water evolution of the slurry decreased rapidly (Figure 2b). With GO content of 0.05% as the turning point, the drop of water extraction rate slowed down after it was greater than 0.05%. Both FA and GO had large surface areas and required more water for the reaction, reducing excess free water. Therefore, the change law of both was consistent. The grout setting time under the synergistic effect of GO-FA

Table 1. The grout setting time of GO-FA synergistic effect.

ID	GO (%)	FA (%)	Initial setting (h)	Final setting (h)	ID	GO (%)	FA (%)	Initial setting (h)	Final setting (h)
0	0	0	12.29	19.59	5	0.05	20	11.58	17.88
1	0.03	10	12.68	17.79	6	0.05	30	12.77	18.29
2	0.03	20	13.09	18.29	7	0.09	10	10.08	15.29
3	0.03	30	13.88	19.33	8	0.09	20	10.65	16.78
4	0.03	10	11.29	16.78	9	0.09	30	11.38	17.09

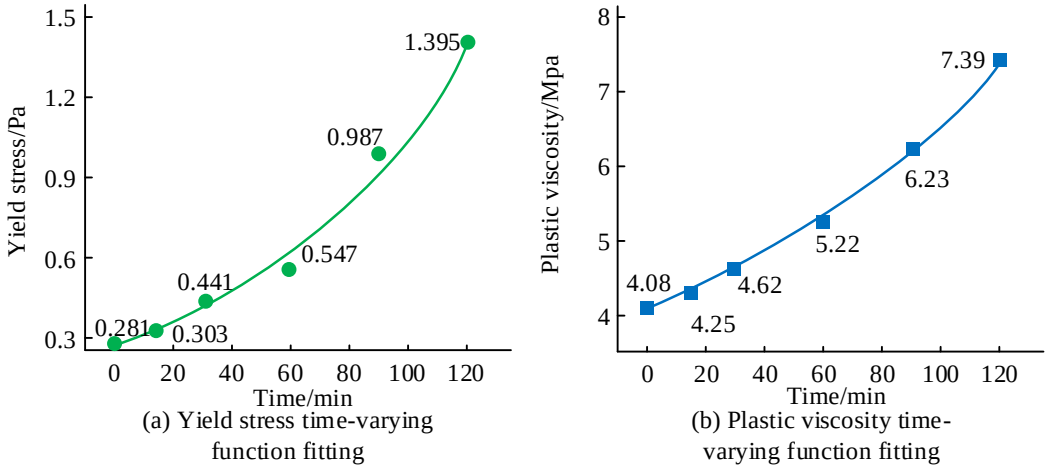

Figure 3. Time-varying function fitting curves of yield stress and plastic viscosity.

was shown in Table 1 with the contents of GO as 0.03%, 0.05%, 0.09% and the contents of FA as 10%, 20%, 30%, respectively. The setting time of GO-FA grout demonstrated significant difference under different GO-FA proportions. The initial setting time was 11.29 h to 13.88 h, and the final setting time was 16.99 h to 19.39 h. Considering the fluidity, stability, setting time, and economy of the slurry, combining 0.03% GO and 20% FA into the slurry could not only ensure the excellent properties of the slurry, but also realize the resource utilization of FA, which met the requirements of low-carbon environmental protection development in the country. The time-varying function fitting curve of yield stress and plastic viscosity was displayed in Figure 3. The yield strength and plasticizing viscosity of the cement slurry after 60 minutes of placement showed a slow rise in the initial stage and a rapid rise in the later stage. Therefore, the rheology of mud had a good correlation with its yield strength and plastic viscosity. The flow performance of cement slurry could be judged by the yield strength and plasticizing viscosity of cement slurry. The yield force and plastic viscosity of the fluid could also be estimated by calculating the macroscopic flow degree of the fluid, so as to study the diffusion of the fluid.

Analysis of mechanical properties and grouting effect of GO-FA new GM

Figure 4 demonstrated the test results of the bending strength of the GO-FA synergistic stone body. The results showed that, when GO was not added, the bending strength of the stone body displayed a decreasing trend when the FA increased. When the FA was 10%, the bending strength of 3, 7, and 28 days decreased by 16.59%, 12.79%, and 10.88%, respectively. When FA content was 20%, the bending strength of 3, 7, and 28 days decreased by 24.67%, 18.11%, and 15.98%, respectively. The bending strength

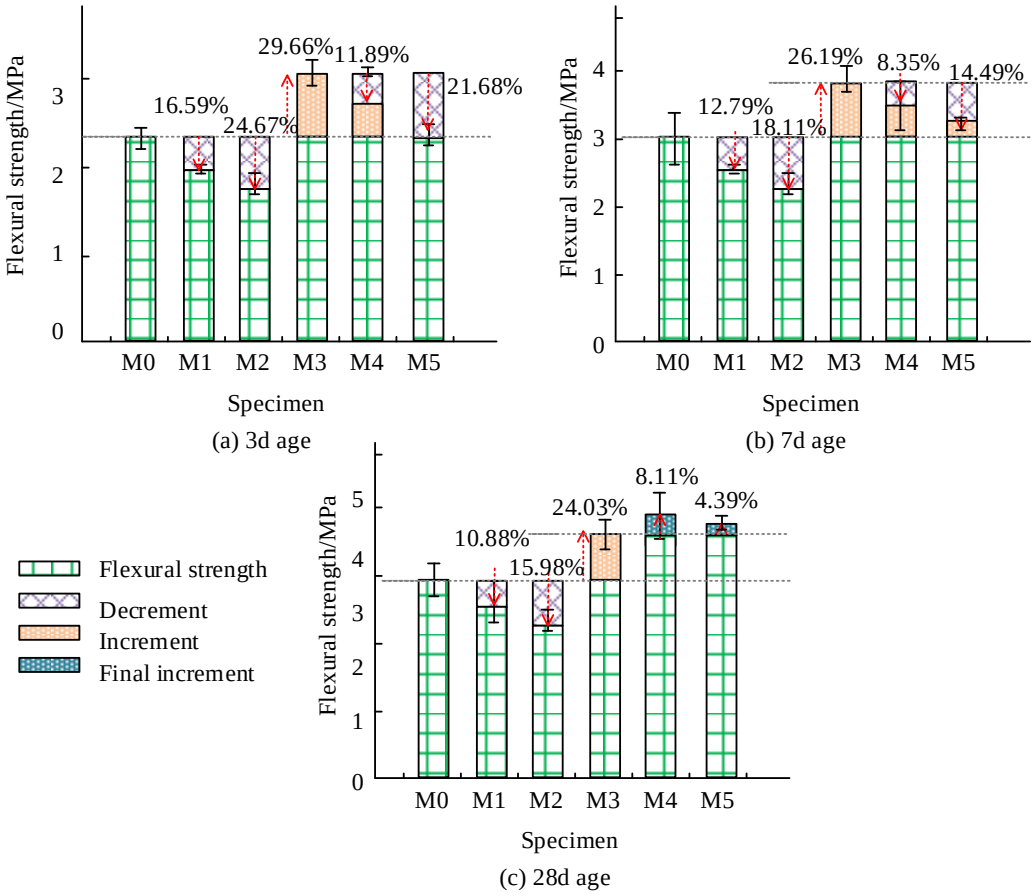

Figure 4. The bending strength of stones under the synergistic effect of GO-FA.

decreased when the FA increased. In addition, the decrease of FA at the young age (3 and 7 days) was larger than that at the old age (28 days), indicating that FA had a deterioration effect. After the addition of GO, the bending strength of the stone body at the corresponding ages was significantly enhanced. At the age of 28 days, when the FA content was 10%, the bending strength was increased by 8.11%, while, when FA content was 20%, the bending strength was increased by 4.39%. The compressive strength of stones under the synergistic effect of GO-FA was shown in Figure 5. When GO was not added, the compressive strength of the stone body demonstrated a decreasing trend when the FA was increased. When FA content was 10%, the compressive strength of 3, 7, and 28 days decreased by 21.97%, 14.88%, and 10.95%, respectively. When FA content was 20%, the compressive strength of 3, 7, and 28 days decreased by 29.56%, 19.59% and 14.01%, respectively. However, after the addition of GO, the stone's compressive strength at the corresponding age was significantly increased with the compressive strength increased by 6.01% when FA content was 10%, and the compressive strength increased by 8.13% when FA content was 20%, respectively at 28 days. The relationship between grouting hardening time and the resistivity of the stone body was shown in Figure 6. The results demonstrated that, with the increase of age, the resistivity of stones with different proportions showed an increasing trend. Before the 8th day, the resistivity increased rapidly with the increase of age, while, after the 9th day, the resistivity slowly increased to a stable value. Overall, GO admixture reduced the resistivity of the stones. On the 28th day of

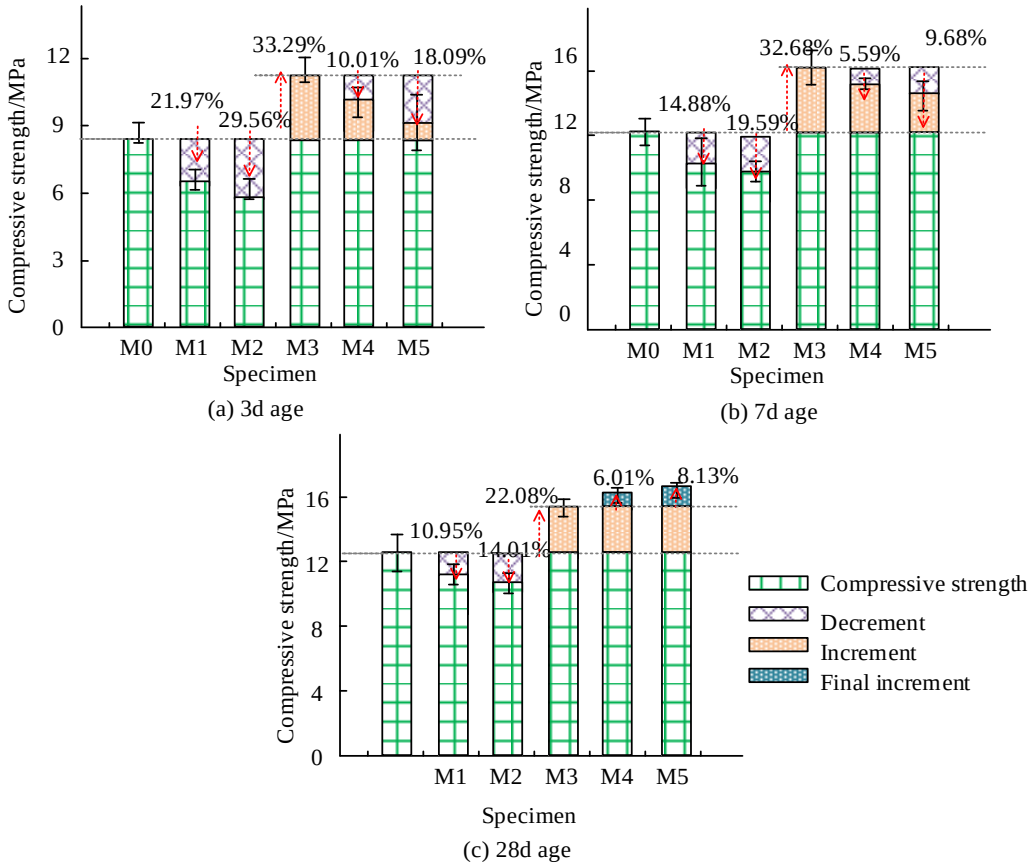

Figure 5. The compressive strength of stones under the synergistic effect of GO-FA.

age, the resistivities of single-doped GO and GO-FA stones were decreased by 12.77% and 7.28%, respectively compared with pure pulp stones. Therefore, the introduction of GO could improve the electrical conductivity of the material.

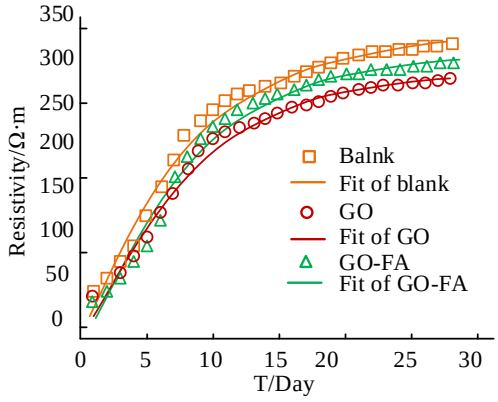

Figure 6. Relationship between grouting hardening time and resistivity of stone body.

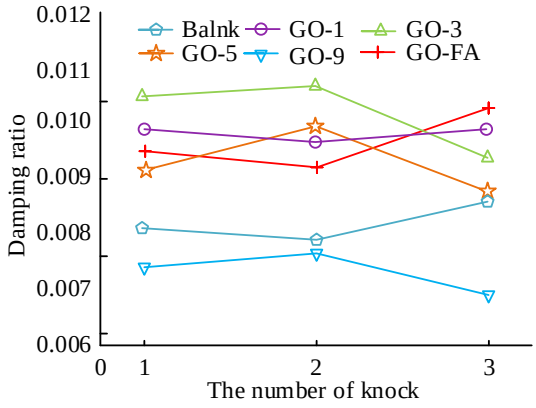

Figure 7. Damping ratio of different proportioning stones calculated by each percussion test.

The damping ratio was calculated by various percussion tests of different proportioned stones (Figure 7). The results showed that the damping ratio values of the same stones were very similar

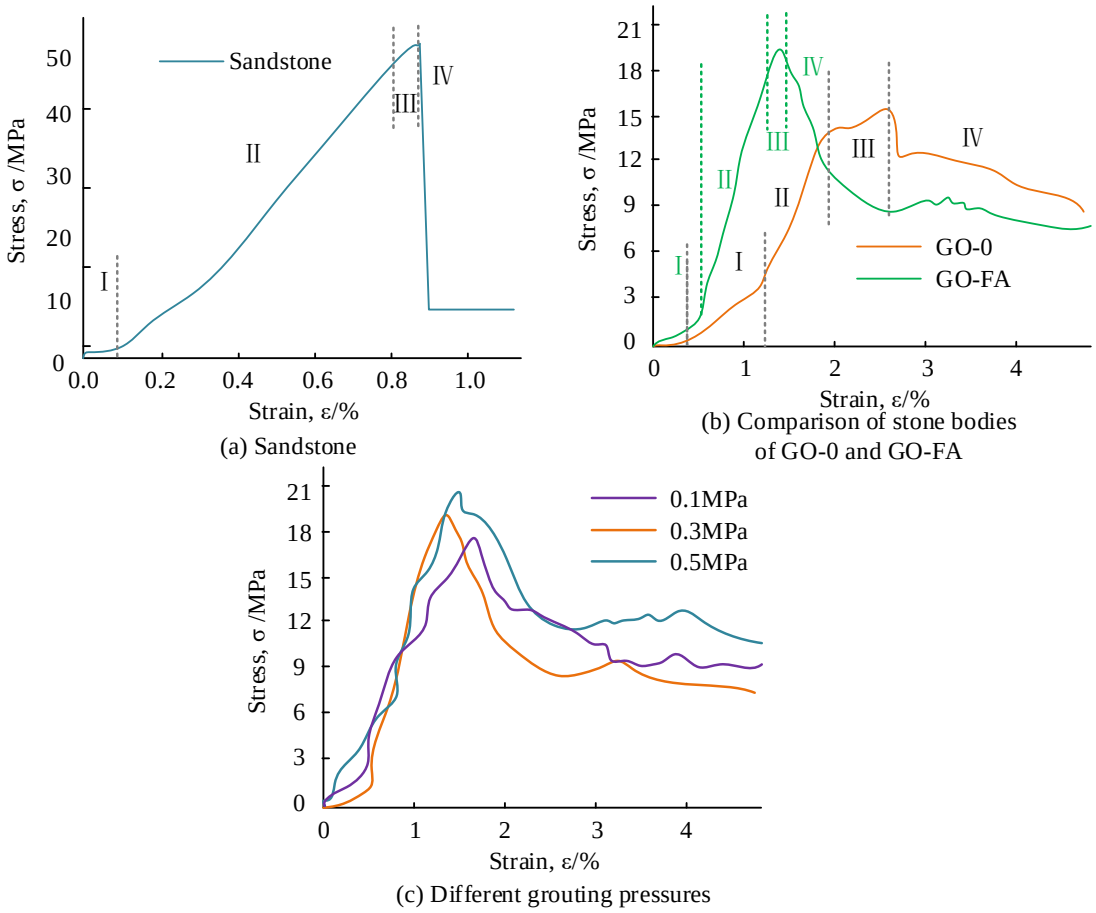

Figure 8. Stress-strain relationship of fractured rock mass by grouting and adding solid.

after 3 knocks, which indicated the accuracy and reliability of the test results. Therefore, the average of the damping ratios could be used as the final damping ratio. When GO dosage was 0.01% and 0.03%, the damping ratio of the stone body was increased by 23.98% and 32.99%, respectively compared with the blank control group. However, with the continuous increase of GO content, the damping ratio of the stone body began to decline. The results confirmed that the damping ratio of cement material could be enhanced by adding GO with the higher the GO content, the greater the increase. The stress-strain relationship between grouting and solid in broken rock mass under intact sandstone and different GM and grouting pressures was shown in Figure 8. The stress-strain relationship curve of sandstone samples was relatively smooth and presented an upward concave distribution. The yield limit strain of GO-0 and GO-FA plus solids was 1.07% and 2.51%, respectively (Figure 8b), indicating that the rigidity of GO-FA plus solids was higher than that of GO-0 plus solids. The ultimate strains of 0.1, 0.3, and 0.5 MPa combined with solids to reach the yield limit were 1.71%, 1.41%, and 1.49%, respectively (Figure 8c).

Conclusion

The frequent occurrence of water-rich and bad geological disasters in underground engineering construction is not conducive to promoting the overall project progress and ensuring the safety of personnel. Grouting is an effective means to

control water-rich and poor geology, but the traditional cement GM has many defects, so a new GO-FA GM was proposed in this study. The material was verified by systematic analysis. The results indicated that the amount of FA and GO influenced the fluidity of the slurry. Adding 0.03% of GO and 20% of FA to the slurry could ensure the excellent properties of the slurry. The time-varying curves of yield stress and plastic viscosity of slurry demonstrated that there was a good correlation between rheological properties of slurry and its yield strength and plastic viscosity. The mechanical property analysis of GO-FA showed that the amount of FA could affect the bending strength, flexural strength, and compressive strength of the final slurry. The relationship between grouting hardening time and rock resistivity indicated that the introduction of GO could enhance the electrical conductivity of the material. The results confirmed that GO-FA plus solid had good rigidity and could be used in the actual construction of underground engineering under the geological condition of poor water richness. Due to limitations of this research, the dispersion of GO was not investigated in this study, which should be the next research direction.

Acknowledgement

This study was supported by National Natural Science Foundation of China (No. 52208358).

References

1. Sun Y, Li G, Zhang N, Chang Q, Xu J, Zhang J. 2021. Development of ensemble learning models to evaluate the strength of coal-grout materials. Int J Min Sci Techno. 31(2):153-162.
2. Di H, Zhou S, Yao X, Tian Z. 2021. *In situ* grouting tests for differential settlement treatment of a cut-and-cover metro tunnel in soft soils. B Eng Geol Environ. 80(8):6415-6427.
3. Hao C, Feng G, Wang P. 2021. Proportion optimization of grouting materials for roadways with soft surrounding mass. Int J Green Energy. 18(2):203-218.
4. Su H, Li R, Yang M. 2021. An experimental study of modified physical performance test of low-temperature epoxy grouting material for grouting joints with tenon and mortise. J Intell Manuf. 32:667-677.
5. Xu J, Kang A, Wu Z, Xiao P, Lu Y. 2021. Research on the formulation and properties of a high-performance geopolymer grouting material based on slag and fly ash. KSCE J Civ Eng. 25(9):3437-3447.
6. Li S, Ma C, Liu R, Chen M, Yan J, Wang Z, *et al*. 2021. Super-absorbent swellable polymer as grouting material for treatment of karst water inrush. Int J Min Sci Techno. 31(5):753-763.
7. Ma S, Ma D. 2021. Grouting material for broken surrounding rock and its mechanical properties of grouting reinforcement. Geotech Geol Eng. 39(5):3785-3793.
8. Zhang J, Li J, Huang C, Chen S. 2022. Study on dynamic viscoelastic constitutive model of nonwater reacted polyurethane grouting materials based on DMA. Rev Adv Mater Sci. 61(1):238-249.
9. Li Z, Liu J, Xu R, Li H, Shi W. 2021. Study of grouting effectiveness based on shear strength evaluation with experimental and numerical approaches. Acta Geotech. 16:3991-4005.
10. Yu Y, Qin Z, Wang X, Zhang L, Chen D, Zhu S. 2021. Development of modified grouting material and its application in roadway repair engineering. Geofluids. 2021:1-15.
11. Guo C, Hu D, Wang F. 2021. Diffusion behavior of polymer grouting materials in sand and gravel. Soil Mech Found Eng. 57:440-444.
12. Zhang P, Su Y, Fan J, Feng H, Shao J, Guo H, *et al*. 2021. Experimental research on the mechanical behavior of grouted sleeves with fiber-reinforced grouting material under cyclic loading. Structures. 34:2189-2204.
13. Zhang C, Shuai B, Jia S, Lv X, Yang T, Chen T, *et al*. 2021. Plasma-functionalized graphene fiber reinforced sulphoaluminate cement-based grouting materials. Ceram Int. 47(11):15392-15399.
14. Yang Z, Zhou S, Li F, Zhang R, Zhu X. 2023. Preparation and rheological performance analysis of volcanic ash and metakaolin based geopolymer grouting materials. Road Mater Pavement. 24(6):1614-1635.
15. Huang Z, Su Q, Huang J, Dong M, Li D, Liu T. 2022. Polyurethane grouting materials with different compositions for the treatment of mud pumping in ballastless track subgrade beds: Properties and application effect. Railway Eng Sci. 30(2):204-220.
16. Nikakhtar L, Zare S, Mirzaei Nasir Abad H. 2020. Numerical modelling of backfill grouting approaches in EPB tunneling. J Min Environ. 11(1):301-314.
17. Dou J, Zhang G, Zhou M, Wang Z, Gyatso N, Jiang M, *et al*. 2020. Curtain grouting experiment in a dam foundation: Case study with the main focus on the Lugeon and grout take tests. B Eng Geol Environ. 79(9):4527-4547.
18. Barma M, Modibbo UM. 2022. Multiobjective mathematical optimization model for municipal solid waste management with economic analysis of reuse/recycling recovered waste materials. J Comput Cogn Eng. 1(3):122-137.
19. Waziri TA, Ibrahim A. 2022. Discrete fix up limit model of a device unit. J Comput Cogn Eng. 2(2):163-167.